

Development of position and pulse shape discriminant neutron detector modules

D.P. Scriven,^{1,2} G. Christian,^{1,2,3} G.V. Rogachev,^{1,2} C.E. Parker,¹ L. Sobotka,⁴ S. Ahn,¹ S. Ota,¹
E. Koshchiy,¹ A. Thomas,⁴ E. Aboud,³ and J. Bishop¹

¹*Cyclotron Institute, Texas A&M University, College Station, Texas 77843*

²*Department of Physics and Astronomy, Texas A&M University, College Station, Texas 77843*

³*Department of Astronomy and Physics, Saint Mary's University, Halifax Nova Scotia, B3H 3C3, Canada*

⁴*Departments of Chemistry and Physics, Washington University, St. Louis, Missouri 63130*

The detection of fast neutrons has many applications: fundamental physics, astrophysics, and stewardship science. In the last year, major strides have been made in the development of a fast neutron detector capable of precise energy measurement. In the 2018-2019 yearly report, we presented the results of both simulation as well as development guided by those simulations [1,2]. The simulations indicated that in order to get the energy resolutions of a few hundred keV, one needs to have position resolution of 2 cm or less with the assumed timing resolution. We since moved forward in the development with those crystals of the solid organic scintillator *p*-terphenyl to create *pseudo-bar* neutron detector modules.

A single pseudo-bar module is quite unique in its design. A module consists of six 2x2x2 cm³ *p*-terphenyl scintillator crystals optically coupled together into a bar with Eljen Technology EJ-550 optical grease. The bar is wrapped in 3M™ Vikuiti™ Enhanced Specular Reflective Film (ESRF) on all four sides along the length. A wrapping of Teflon is then applied to mechanically secure the crystals and to bind the ESRF to the scintillator faces. A Hamamatsu R1450 photomultiplier tube (PMT) is placed at each end of the bar for light readout.

By looking at energy and timing measurements from the two PMTs (*left* and *right*) we can extract position information from the bar as is typically done. Shown in Fig. 1 (left) is the position separation

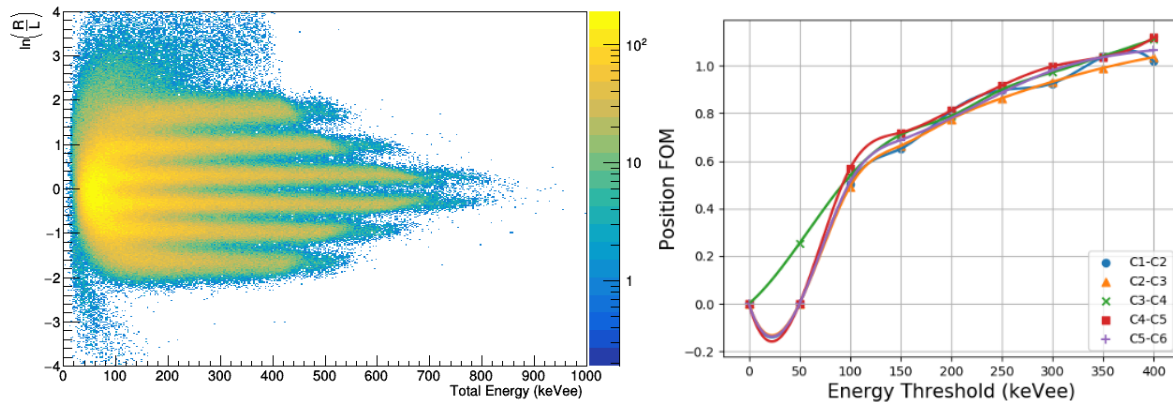


Fig. 1. Exposing the pseudo-bar to a ²⁵²Cf source we show (left) the energy dependence on crystal distinguishability is shown here by plotting $\ln(E_R/E_L)$ vs. E_{total} . At low energy it becomes more difficult to discriminate between crystals. (right) The FOM profiles for each neighboring pair of crystals. The FOM=0 points at low energy are present where no distinguishability exists.

parameter $\ln(E_R/E_L)$ measured from the two PMTs as a function of energy. The separation parameter is the primary component used for crystal distinction. Each peak in the *y*-axis projected spectrum

corresponds to a single crystal in the pseudo-bar. We define a figure-of-merit (FOM) which allows us to quantify the discrimination between each peak,

$$FOM_{i,i+1} = \frac{\mu_{i+1} - \mu_i}{2.355(\sigma_i + \sigma_{i+1})} \quad (1)$$

Here, μ and σ are the mean and standard deviation from the Gaussian fit of each distribution. If labelling the crystals 1-6, the FOM is calculated for each pair of neighboring distributions. Looking at the 1D spectrum with cuts on energy of 50 keVee, the FOM is calculated for each bin, generating FOM profiles shown in Fig. 1 (right). These profiles give a detailed look at how distinguishable each peak is. Via its definition, a FOM=1 indicates the crossing point of the two Gaussians to be at the $2\sigma\sqrt{2\ln 2}$ level (>97%). This shows that position discrimination is capable above 300 keVee with high confidence.

In the presence of a neutron field, there nearly always exists a γ -ray field as well. Most neutron detectors are sensitive to both radiations. Some scintillators including *p*-terphenyl are capable of pulse shape discrimination (PSD) which allows for *n*/ γ particle identification. We expose the pseudo-bar to a ^{252}Cf source to establish the quality of PSD in the pseudo-bar. The PSD quantity is calculated by taking two integrations of the scintillation pulse. The first integration is over the total waveform, and the second is over the tail. PSD is the ratio of the tail integration over the total integration.

In order to quantify the PSD, one again establishes a FOM. The FOM takes the same form as Eq.(1), were i and $i+1$ become γ and n respectively. We then calculate the FOM for each crystal by again making 50 keVee bins in the 1D PSD spectrum (γ -projection of Fig. 2). The PSD profiles indicate that separation of >97% is achievable in all crystals below 150 keVee, and in some crystals as low as 100 keVee.

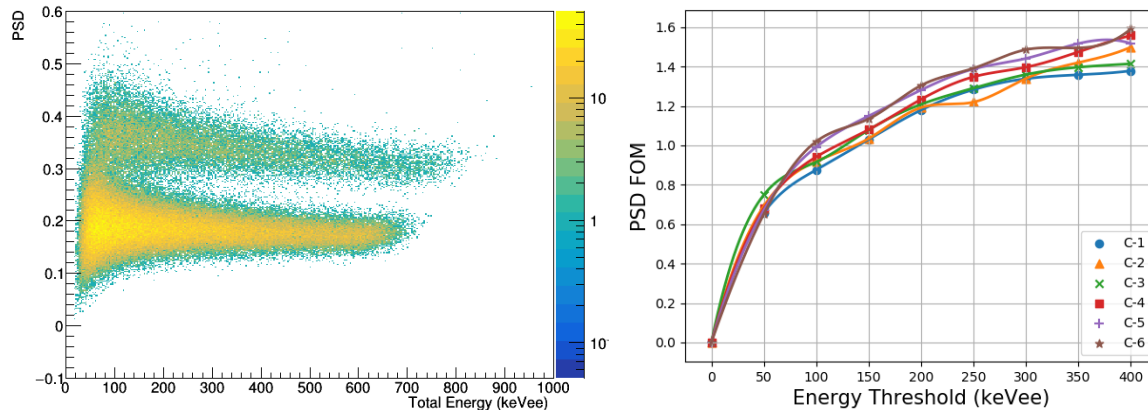


Fig. 2. (left) A typical 2D PSD spectrum. The PSD vs total energy shows the energy dependence of the PSD. The spectrum shown is from one of the central two crystals in the pseudo-bar C-3 which has the worst PSD of the few crystals. The top band corresponds to neutrons while the bottom band is γ -ray detections. (right) The PSD FOM profiles for each crystal.

With the energy dependence understood, we can look at the position discriminating parameter with the PSD parameter. Shown in Fig. 3 is the PSD vs position parameter. Here, a cut is made at 300 keVee as prescribed by the position FOM profiles in Fig. 1. There is clear position and n/γ discrimination for each crystal.

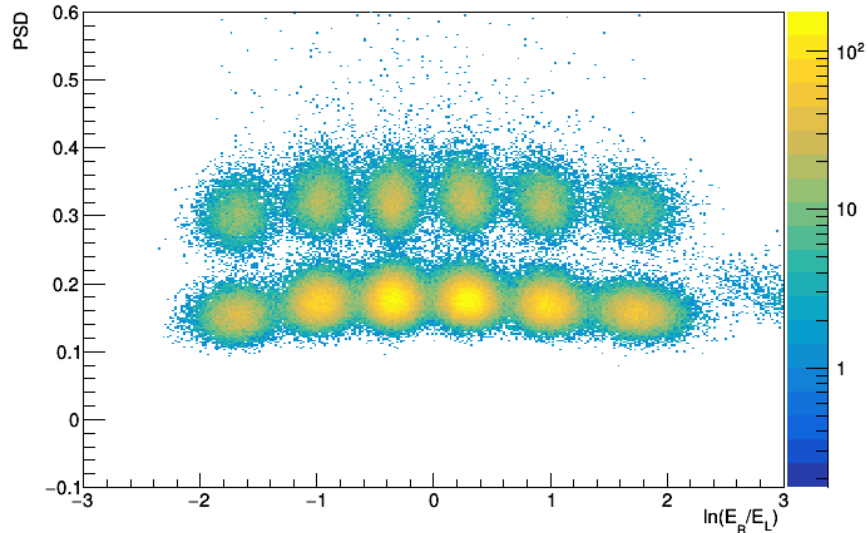


Fig. 3. Shown together is the PSD vs the position separation parameter. Here, a cut is made to exclude events at 300 keVee or less. The top band again corresponds to neutrons while the lower band corresponds to γ -ray detections.

To conclude, a neutron detector module has developed which can be used for the detection of fast neutrons with good spatial resolution and n/γ PSD below 300 keVee. We are currently working to measure the timing resolution of a module. We are continuing with the construction of a prototype array consisting of ~ 40 pseudo-bars due for commissioning in 2020, followed by addition of more modules to a full scale detector consisting of 128 pseudo-bars.

- [1] D.P. Scriven *et al.*, *Progress in Research*, Cyclotron Institute, Texas A&M University (2018-2019), p. IV-55.
- [2] C.E. Parker *et al.*, *Progress in Research*, Cyclotron Institute, Texas A&M University (2018-2019), p. IV-52.